

Insights into statistical structural characteristics and deformation properties of columnar jointed basalts: field investigation in the Baihetan Dam base, China

Jie Cui¹ · Quan Jiang¹ · Xiating Feng¹ · Shaojun Li¹ · Junfeng Liu² · Wenfu Chen² · Jiancong Zhang¹ · Shufeng Pei¹

Received: 20 June 2016 / Accepted: 28 February 2017 / Published online: 20 March 2017
© Springer-Verlag Berlin Heidelberg 2017

Abstract The columnar jointed basalt (CJB) in the left-bank dam foundation of the Baihetan hydropower station, China, is a special jointed rock mass with a columnar cylinder structure. A field investigation revealed three types of joints developing in the CJB: (1) columnar joints, (2) internal steeply dipping joints (ISDJ), and (3) internal gently dipping joints (IGDJ). A uniform distribution survey lines method (UDSLM) is proposed to describe quantitatively the spatial structural features of CJB exposed in limited outcrops. The visible spacing of internal joints in CJB is found to evolve; joint spacing decreases with increased degrees of weathering, disturbance, and time after unloading excavation. Combined with the actual structure, the formation mechanism of CJB is discussed from the structure of a single column to the whole rock mass, based on the contraction hypothesis. A columnar joint tensor, which is closely related to the CJB deformation characteristics, is established for describing the complex columnar joint network in the three-dimensional space based on the measurement data with the UDSL. In addition, the structural characteristics of intact columns were exposed through dismantling cuboid specimens of 0.5 m edge lengths and 1.0 m height, verifying the rationality of the UDSL and the evaluation of structural characteristics of CJB in the Baihetan dam foundation. This in situ study presents an in-depth understanding of CJB

structure and provides meaningful guidance for excavation and supporting reinforcement for the CJB exposed on the Chinese Baihetan dam foundation.

Keywords Columnar jointed basalt · Irregular structural feature · Internal joint · Deformation anisotropy · Unloading excavation · Columnar joint tensor

Introduction

Discontinuous structural planes widely develop in a rock mass after complex diagenetic and mineralization processes and supergene evolution. Compared with the generally continuous, homogeneous, isotropic, and linear elastic material, rock mass exhibits extremely complicated mechanical behavior characterized by discontinuity, inhomogeneity, anisotropy, and non-linear elasticity (DIANE) (Sun 1993; Hudson and Harrison 2000; Wang 2009). A columnar jointed rock mass (CJRM), formed by condensation and contraction of lava flows (Spry 1962; Reiter et al. 1987; Grossenbacher and McDuffie 1995; Phillips et al. 2013), is a typical DIANE material and widely distributed in the nature. The typical CJRM has significant structural characteristics, as it is composed of prismatic blocks cut by multiple sets of joints with approximately parallel intersecting lines. From a structural perspective, a columnar joint system is more regular than a random joint system and more complex than a stratified rock mass. The typical CJRM is represented by the Giant's Causeway in Northern Ireland and the Scottish island of Staffa, as shown in Fig. 1 (Goehring 2013; Phillips et al. 2013).

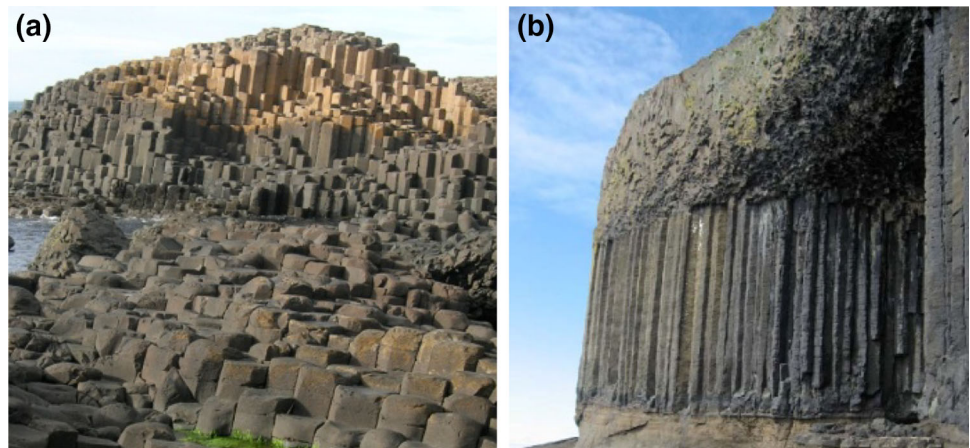
As a consequence of the recent construction of large-scale hydroelectric projects in China, CJRM has been gradually revealed as an engineering rock mass, and has

✉ Quan Jiang
qjiang@whrsm.ac.cn

¹ State Key Laboratory of Geomechanics and Geotechnical Engineering, Institute of Rock and Soil Mechanics, Chinese Academy of Sciences, Wuhan 430071, Hubei, China

² China Three Gorges Project Corporation, Beijing 100038, China

Fig. 1 Typical CJRM in natural environments. **a** Northern Ireland giant dikes (Goehring 2013); **b** Scottish island of Staffa (Phillips et al. 2013)



thus caught the attention of researchers because of its special structure and mechanical properties, which are closely related to the stability of slopes and tunnels. Most of the current studies on CJRM have covered formation mechanisms (Reiter et al. 1987; Müller 1998a, b; Hull and Caddock 1999; Goehring et al. 2009; Hetényi et al. 2012; Goehring 2013; Phillips et al. 2013), geometrical modeling (Zhu et al. 2009; Zheng et al. 2011), scale effects (Liu et al. 2009; Zhu et al. 2009; Di et al. 2011a), constitutive relationships (Di et al. 2011b; Shan and Di 2013), and failure mechanisms (Zhu 2010; Jiang et al. 2014; Jin et al. 2015). Discussions in those studies have mainly focused on the typical CJRM with regular and intact columnar structures owing to a deficiency of detail in situ statistical data. However, actual columns always appear irregular and have intensively internal secondary joints, which have a significant impact on the CJRM mechanical properties, as a result of the lack of sufficient and stable formation conditions. Further in-depth investigation of the geometric and mechanical properties of an irregular CJRM is still necessary.

Conventional rock mechanics emphasize that joints control the mechanical response of the rock mass by introducing strong anisotropic effects (Hudson and Priest 1983; Singh et al. 2002; Brady and Brown 2013; Barton and Quadros 2014). The structure of CJRM controls the deformation anisotropy and failure behavior. Objective and quantitative estimations of the anisotropic properties based on rock mass structural characteristics are very important for the accurate deformation analysis. A discrete element numerical model with regular column shapes is universally adopted in numerical computations to study deformation anisotropy of CJRM (Zhu et al. 2009; Xu et al. 2010; Di et al. 2011a, 2013). However, the analytical process is disconnected from the actual measured data of columnar joints exposed in situ, and fails to reflect the irregularity of columns and internal joints, which are critical to comprehending the actual deformation properties of CJRM.

Therefore, it is necessary to establish a field measurement method applicable to CJRM with variously exposed characteristics and an analytical method for anisotropic properties based on those field data.

This paper deeply investigates the columnar jointed basalt (CJB), which is here exposed on the left-bank dam foundation of the Baihetan hydropower station, for the purpose of analyzing the column structure, and inferring statistical characteristics of a columnar joint system. Through in situ statistical observations, borehole camera technology, and scanning electron microscopy (SEM), the evolution of the visible spacing of the internal joints is revealed. A uniform distribution survey lines method (UDSLM) is put forward to quantitatively describe the spatial structures of an irregular CJB exposed in a limited outcrop. Finally, on the basis of the crack tensor theory and measurement data, an in-depth analysis of the anisotropic deformation characteristics and failure behavior of the CJB is carried out.

Engineering background

The Baihetan hydropower station under construction is located at the border between the Ningnan County of Sichuan Province and the Qiaojia County of Yunnan Province downstream of the Jinsha River. This area is characterized by highland and ravine landforms. The Baihetan hydropower station will be the second-largest hydropower station after Three Gorges in China, possessing more than 1000×10^4 kW of installed capacity (Dai et al. 2016). The Permian Emeishan Group ($P_2\beta$) basalt originated from magmatic and volcanic eruptions underlies the study area. Strata is inclined, with strikes trending $N30^\circ-50^\circ E$ and dip angles of $15^\circ-25^\circ$. The surface layer is Quaternary loose deposits (Q4). The engineering region is divided into 11 basalt flow layers ($P_2\beta_1-P_2\beta_{11}$) according to the number of intermittent eruptions.

The barrage will be a 289 m concrete double-curvature arch dam. Figure 2a shows the left-bank abutment slot excavation. The CJB developed in the $P_2\beta_3^3$ lava flow deposits, which outcrops at 570–670 m on the left-bank dam foundation surface and at 545–600 m on the right bank (Xu et al. 2015a). The column axis direction is almost perpendicular to the lava flow. Since the tendency of the surface of dam foundation that is about 119° – 129° is benefit to the dumping of columns whose axis pitch direction is about 310° , and a large area of CJB is exposed in the excavation area, the CJB shows serious deformation and unloading failure. As a result, our focus is on the left bank CJB (Fig. 2a). The column forms exposed on the dam foundation surface are irregular, with intensely developed internal joints, unlike typically regular CJB (Fig. 2b). The rock mass exhibits low-integrity mosaic block structure. After excavation unloading, severe cracking of CJB emerges along different joint surfaces (Fig. 2c), which causes the sprayed concrete layer to crack (Fig. 2d). The horizontal deformation modulus of the CJB protolith in the left bank is about 7–11 GPa and 5–9 GPa in the vertical direction by rigid bearing plate tests. In contrast, the deformation modulus of rock mass in the relaxation layer in both horizontal and vertical directions drop to 3.01–5.19 GPa (Xu et al. 2015b). In addition, the general relaxation depth of post-excavation rock is 1.6–3.6 m and locally up to 4 m, with a 3000–3800 m/s acoustic wave velocity, which is about 30 % lower than that of the original rock mass (Xu et al. 2015b; Feng et al. 2015). The exposed characteristics and measured data indicate that the CJB possesses a poor anti-deforming capability and serious

unloading damage influenced by excavation. Therefore, the structural features and deformation-failure mechanisms of the CJB need to be thoroughly analyzed for reasonable evaluation for whether the rock can meet the strict deformation requirements of a high arch concrete dam foundation, which is essential for the stability and long-term operational safety of the dam (Yang et al. 2010; Salazar et al. 2016).

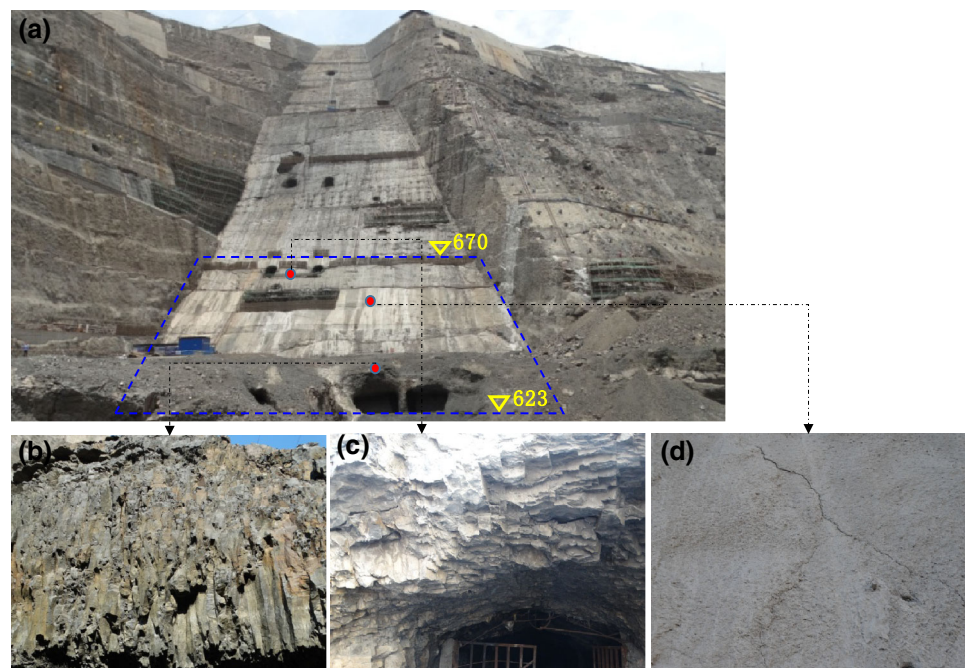
CJB structure features

Joint types

The specific geometric distribution of joints molds the basalt into a mosaic block structure, which is closely related to the formation mechanism of columnar joints (Hetényi et al. 2012). In situ observation reveals that the columnar joint system consists of three types of dominant joints—columnar joints, internal steeply dipping joints (ISDJ), and internal gently dipping joints (IGDJ), as shown in Fig. 3. The geometrical structure of the CJB is objectively described and the origins of the structures are considered based on the contraction hypothesis in combination with field observations, SEM, and previous research.

The CJB in the left-bank dam foundation has distinct partition structure features. With the increase of the depth in the direction perpendicular to the strata, shape of columns transform from irregular to regular. The upper part of the CJB located near the base surface is characterized by curved columnar joint planes, poor extensibility, obscurity

Fig. 2 CJB outcrop feature of the left-bank dam foundation. **a** Excavation appearance of left-bank abutment slot; **b** the exposed CJB with irregular column structure; **c** cracking of CJB along joint surfaces; **d** cracking of sprayed concrete layer on the dam surface



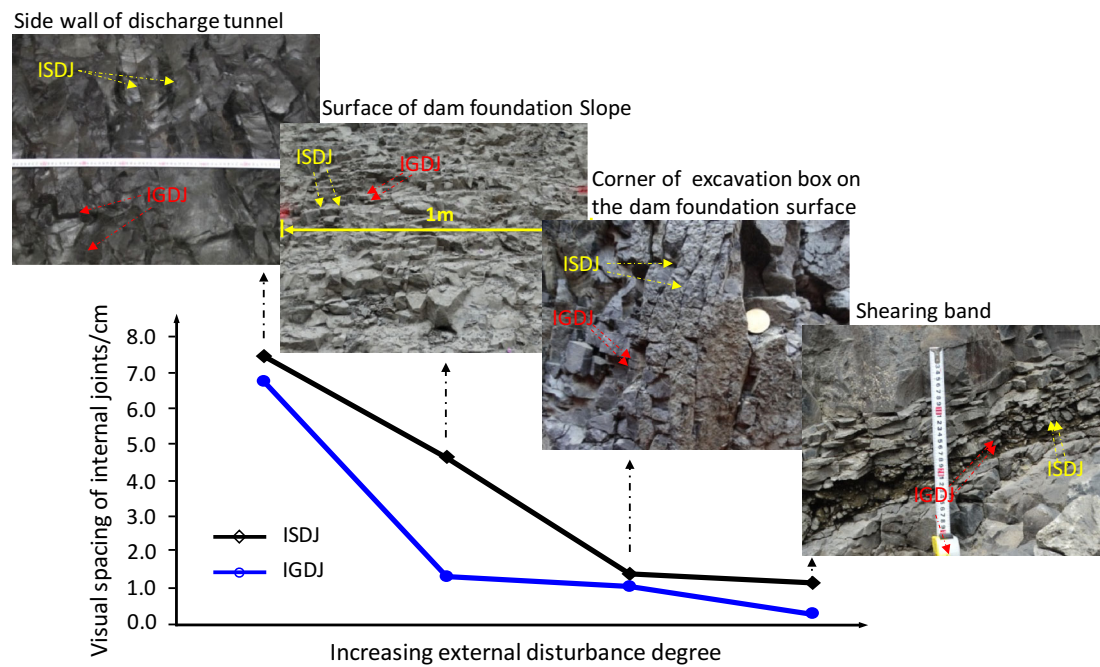


Fig. 3 Evolution of internal joints inside CJB with different degrees of weathering and disturbance

of intersecting ridgelines of adjacent columnar joint planes with arc-shaped connections, size variability of column cross-sections in the axis direction, and intensive development of internal joints, especially for IGDJ. In the deeper strata, the CJB possesses a straight columnar joint surface, better extensibility, uniform column cross-sections along the axial direction with regular column shapes, better integrity, and a significantly decreased internal joint development, in comparison with the irregular CJB. The internal joints develop in the columns in a certain regular way. ISDJ are approximately parallel to the column axis and are characterized by smooth and wavy shaped surfaces. The IGDJ, whose surfaces are smooth and flat, develop perpendicularly to the column axis.

Evolution of internal joint spacing

Multi-scale field observation shows that the visible spacing of internal joints evolves notably after unloading excavation. When the unloading disturbance, weathering, and alteration intensify and time passes, the visible spacing of internal joints gradually decreases. IGDJ spacing is particularly prominent. Figure 3 shows the spacing of internal joints varies with the different degrees of external disturbances. The macroscopic spacing of fresh CJB reaches approximately 7 cm in the discharge tunnel and decreases with increasing weathering and disturbance degrees. In the areas of strong weathering where groundwater develops and stress is severely perturbed, such as around shearing bands, the visible spacing of ISDJ and IGDJ decreases to 1.2 and 0.36 cm, respectively, and columns are

cut into fragmented blocks. In contrast to the IGDJ, the ISDJ spacing gradually stabilizes and exhibits a weaker evolution under the weathering and disturbance. The results of borehole camera observations around the dam foundation surface indicate that the internal joints continually appear and open after the excavation until converging to a stable arrangement (Fig. 4). Considering the evolution of internal joint spacing, the reduction in dynamic disturbances and introduction of timely support are vital to the integrity and stability of the CJB near the dam base surface.

The evolution mechanism of IGDJ is explored through SEM of irregular and regular columnar jointed rock blocks (Fig. 5). The results show that it is the microscopic layered structure along the column axis that causes the significant evolution effects of IGDJ spacing. Under the influence of external disturbances, the gradual connecting of layered structures prompts the formation of joints that are visible to the naked eyes and lead to decreased spacing. The spacing can be very small, provided that the weathering and disturbance are strong enough. Furthermore, the more evident layered structure of irregular columns compared with the regular columns makes the formation of visible joints in an irregular CJB easier under the same conditions, which explains why the development of IGDJ in irregular columns is denser. Therefore, the structure of CJB is native and specific. Later alterations, such as disturbance, weathering, and aging, cause the intrinsically damaged surfaces to interconnect and open to form visible joints. The CJB develops greater tendency for cracking because of the evolution of internal joints.

Speculation on the formation mechanism

On the basis of the contraction hypothesis, we speculate on the formation mechanism of CJB in the dam foundation by integrating previous research (Spry 1962; Reiter et al. 1987; Budkewitsch and Robin 1994) and assessing the

limited exposed features and the corresponding microstructural features. This work is expected to offer some reference for the analysis and explanation of the regional structural characteristics of the CJB.

The CJB is the product of lava flow contraction under comprehensive conditions including lava material composition, geometric constraints, and heat exchange conditions (Reiter et al. 1987). Different formation conditions contribute to the structural diversity of column shapes, joint surface properties, and joint densities (Degraff and Aydin 1993; Grossenbacher and McDuffie 1995; Hetényi et al. 2012). In the process of dynamic adjustment to balance the temperature field between molten lava, atmosphere, and bedrock, the tensile stress accumulated during the heat transfer and release results in the formation of complex columnar joint systems.

The geometric boundary of the CJB in the dam foundation is controlled by the monoclinic terrain (Hetényi et al. 2012). The lava flow thickness is uniform and the occurrence is consistent with the terrain before its formation. In the geological setting, the interfaces between the lava flow and atmosphere, as well as the lava flow and bedrock, become the initial boundaries of the heat exchange (Fig. 6). In a cross section perpendicular to the column axis, tensile cracks are generated surrounding the countless regularly arranged shrinkage centers and form polyhedral columns (Müller 1998b). During the initial condensation, the temperature gradient is large near the temperature controlling boundary, where a large tensile stress accumulates to form columnar joints with flat and rough surfaces, as described by Eq. (1) (Spry 1962; Hetényi et al. 2012).

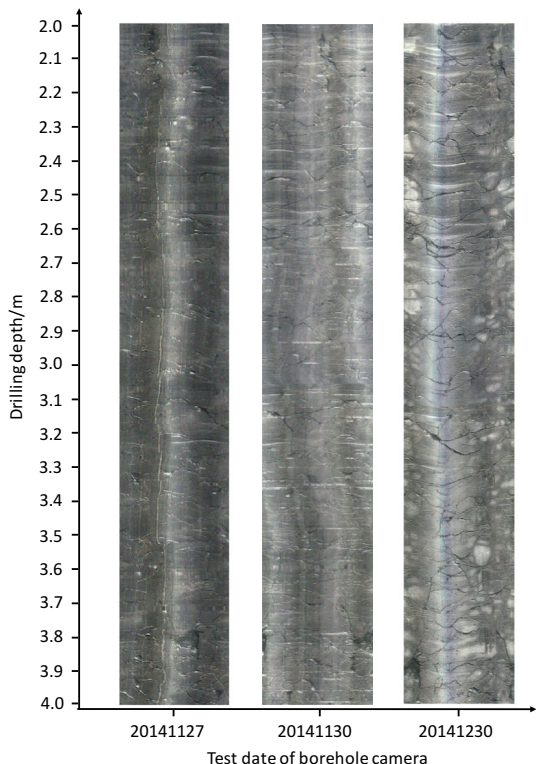


Fig. 4 Evolution of internal joints with time after excavation of dam base

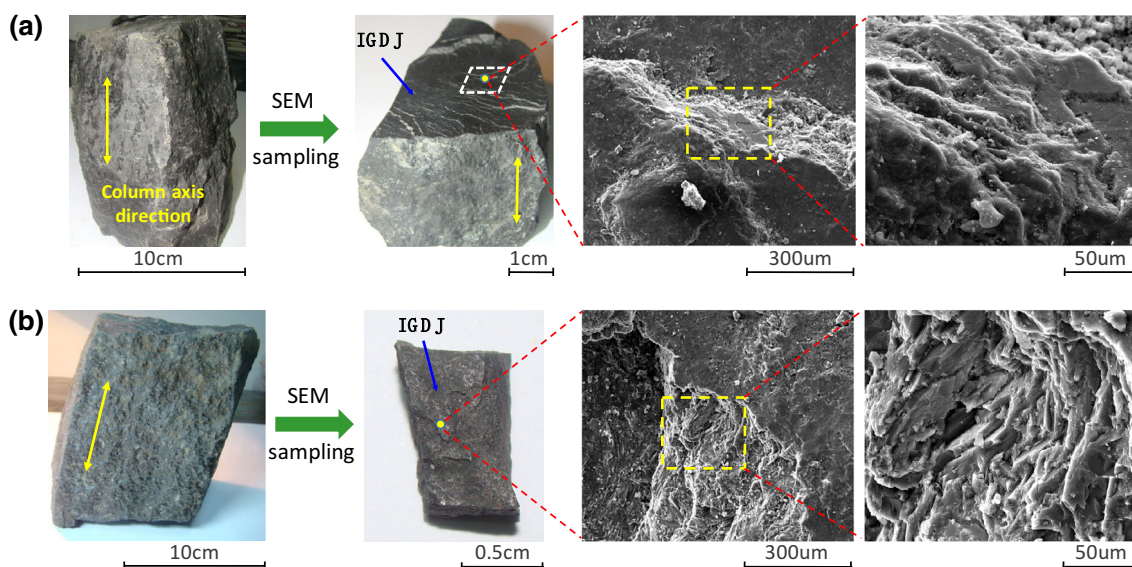
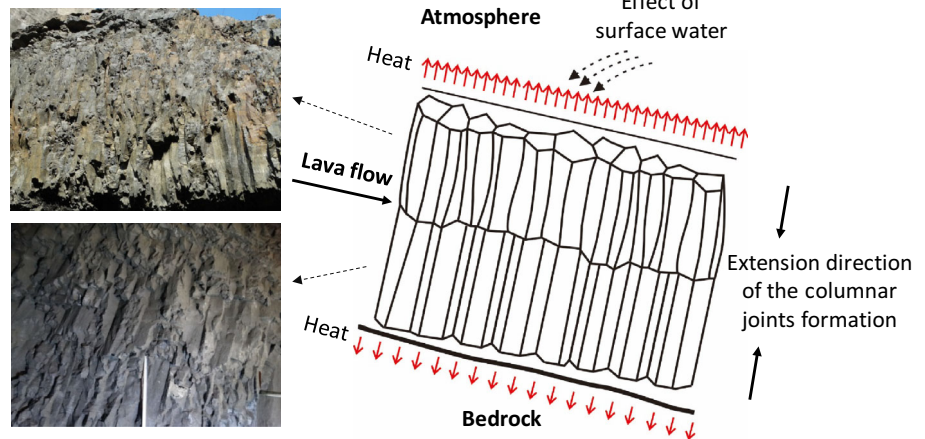


Fig. 5 Specific surface patterns of IGDJ observed by SEM **a** IGDJ of the irregular column; **b** IGDJ of the regular column

Fig. 6 Macroscopic partition structure of columnar jointed basalt



$$\sigma_{th} = E \cdot \alpha \cdot \Delta T / (1 - \nu), \quad (1)$$

where σ_{th} is the thermal stress that accumulates due to the shrinkage resulting from cooling, E is the elastic modulus, ν is the Poisson ratio, α is the coefficient of thermal expansion, and ΔT is the temperature difference between external temperatures (air, water, host rock) and the glass transition temperature T_g , i.e., the temperature below which the rock is able to build up stresses (Zarzicky 1982).

The cooling rate is high in the upper part of the lava flow because heat exchange is rapid when surface water plays an important role in promoting condensation and contraction. The relatively unstable state of the condensation and contraction system generates the irregularity of the columns. In contrast, cooling in the deep part of the lava bed eases without the influence of surface water and pressing heat transfer conditions (Fig. 6). The relatively stable state makes it possible fully to form more regular and intact column structures (Phillips et al. 2013).

Part of the lava heat releases in the form of stress during the formation of columnar joints. However, insufficient heat dissipation means some part of the heat remains in the columns, which needs further transfer and release. At this point, the columnar joint surfaces, as lower energy regions, construct new geometric control boundaries for the new local temperature fields. The dense internal joints are the products of the adjustments of the in-column temperature fields. In the upper irregular columns, much residual heat aggregates as a result of the rapid contraction and leads to internal cracking of the columns under further condensation. For the deep lava, however, heat adequately releases by heat exchange and crystallization. The density of internal joints is relatively small in these columns because there is less residual heat accumulation in the columns. In the local temperature field, the scale of heat transfer in the direction perpendicular to the column axis is controlled by the column diameter. Larger multidirectional tensile stresses are accumulated and promote the formation of several ISDJ sets.

ISDJ formation is a gradual process of external to internal promotion by heat transfer along the column axis. In the axis direction, heat transfers from the lava to the atmosphere and bedrock; the thickness of lava flow dictates the scale of heat transfer. Larger transfer scales make lava condensation and contraction relatively slow and steady. The temperature gradient caused by the movement of isothermal surface leads to layered damage and constitutes a layered structure. As the gradient of heat adjustment inside the columns is far less than the temperature gradient in the columnar joint formation process, the corresponding tension stress is relatively smaller. The surface morphology of internal joints is smooth compared with columnar joints because of a gentler formation process.

Figure 7 illustrates the formation mechanics of the internal joint system as speculated above, and the correspondence between the actual exposed occurrences of internal joints and columnar joints verifies the speculation of the formation mechanism of the internal joints to a certain extent. In the columns, every newborn crack will become the control boundary for the next transfer and dissipation of energy. The lava heat transfers and releases in the form of tensile stress accumulation and release, and the process of lava condensation and contraction causes continual damage to the rock. As the temperature gradient weakens and the temperature control borders change, the damaged form gradually weakens and changes from visible columnar joints to internal joints with better connectivity, to closed internal joints with poorer connectivity. Eventually, tensile fractures are unable to form, which means the energy exchange between the lava and its surroundings has approached equilibrium. There is an order of priority during the formation of columnar joint systems. A columnar joint forms first and creates the thermal boundary conditions for the internal joints. However, the boundary cannot be clearly defined. The whole formation process advances step by step from the interfaces between the lava and

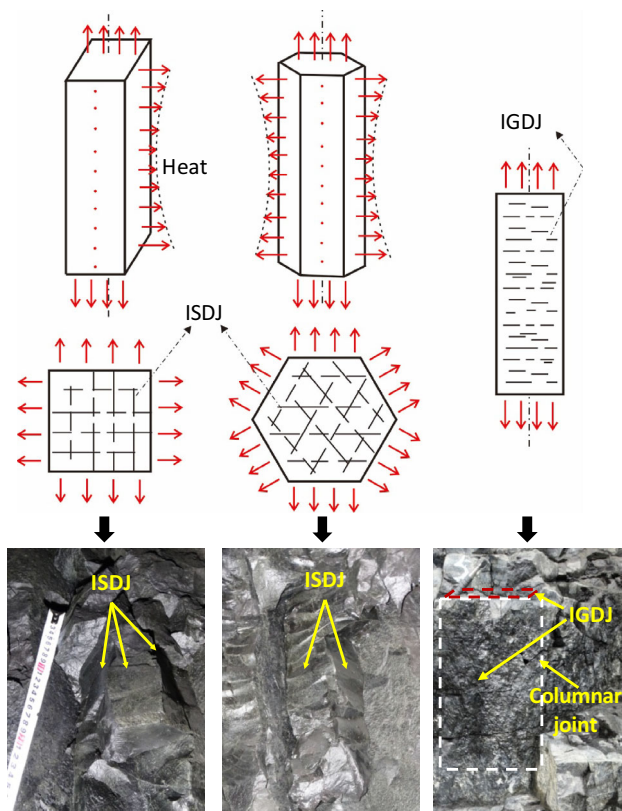


Fig. 7 Speculation about the formation mechanism of internal joints

atmosphere, and the lava and bedrock to the lava interior. The mechanical properties of different joint types have obvious differences because of their priority level in the formation process. Columnar joints created by the accumulated tensile stress with larger temperature gradients represent the most serious injuries with relatively poor mechanical properties. The internal joints take second place, which is consistent with the progressive failure characteristics along the joints of the CJB. Under the weathering and disturbance, the damage to internal joints is further intensified. The influence of internal joints on the rock mass cannot be ignored. The outcrop features of columnar joints near the dam foundation plane reveal that the column irregularity, intensive internal joint development, and unstable condensation and contraction processes are relevant. The integrity of the column structure is therefore closely related to the stability and sufficiency of the condensation and contraction process.

Statistical analysis of CJRM geometric features

The above analysis of the CJB structure clearly reveals the developed characteristics of the joint types, joint set number, joint orientation, and spacing. On this basis, the targeted statistical measurement of the geometric

characteristics of the columnar joint system is carried out for the quantitative evaluation of CJB mechanical properties.

Geometric characteristics of columnar joints

The irregularity of the CJB is mainly reflected in the diversity of column cross-section shapes and the variability of column cross-section size along the axis of the columns. A pole and contour plots diagram is used to describe accurately the distribution characteristics of columnar joints.

Under the limited exposed conditions at the site, fully exposed columns are unavailable for measurement, including any fully exposed cross-sections of the columns. It is, therefore, impossible to obtain large amounts of statistical information of the CJB structural characteristics through direct measurement of the entire column. According to the construction environment, the tunnel walls are the maximum area to reveal the measurable columnar joints as a consequence of the excavation of the experiment tunnels and exploratory caves. Both sides of the tunnel walls provide effective measurement points. Thus, one survey line can reveal four effective surfaces of the columns for measuring. Because the average polygonal order of the column cross-section is below six (Hetényi et al. 2012), three uniformly distributed survey lines can guarantee the six surfaces of the columns in different directions are available for measurement and the measurement frequency of each surface is about the same. The one experiment tunnel and two exploratory caves orientated 10° , 65° , and 126° , respectively, serve as the three survey lines (see Fig. 8a). The attitudes of every exposed columnar joint and the spacing of column traces on both excavation walls along the survey lines are measured, as illustrated in Fig. 8c.

Orientation of columnar joints

Equal sized measurement samples were randomly drawn from the three survey lines and analyzed to ensure the objectivity and rationality of the orientation features of the dominant columnar joint sets. Results were expressed on a polar equal angle net (Fig. 9a). The heterogeneity and asymmetry of pole distributions indicate the non-uniformity of column cross-section shapes. The 360° distribution of poles indicates that column cross-sections vary along the column axis and the column ridgelines are not strictly parallel to the column axis. These characteristics are in accordance with the column forms revealed by excavation. Therefore, a regular hexagonal prism cut by three dominant joint sets with fixed orientations cannot truly reflect the irregular column forms.

Fig. 8 Measurement of columnar joints. **a** Arrangement of survey lines; **b** column diameter correction; **c** Measurement of columnar joint occurrence and trace spacing

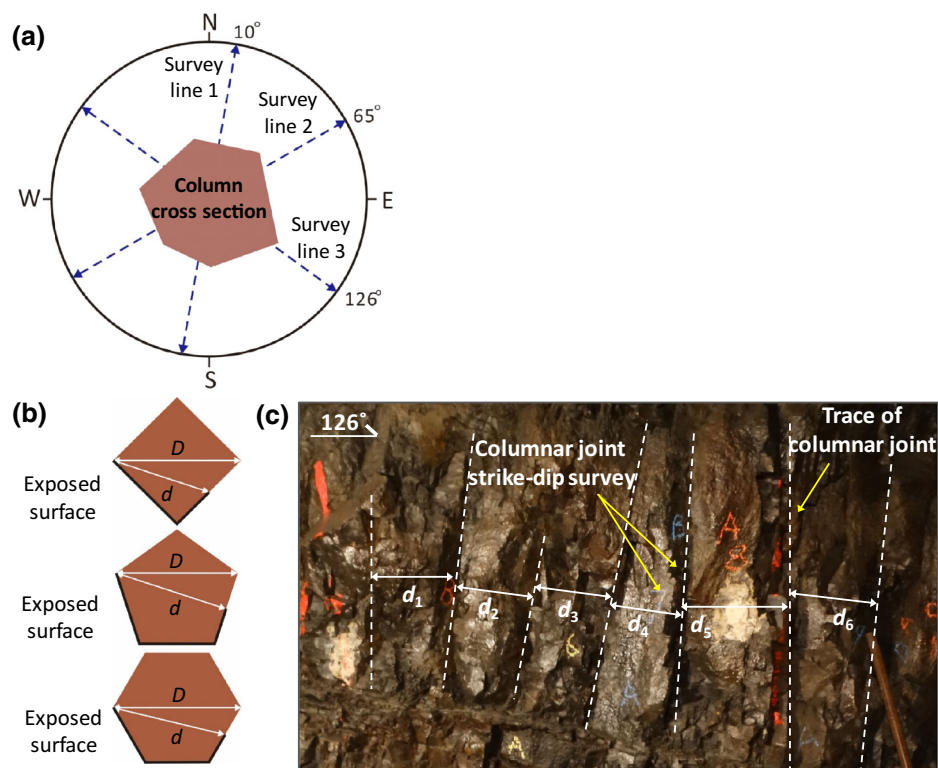
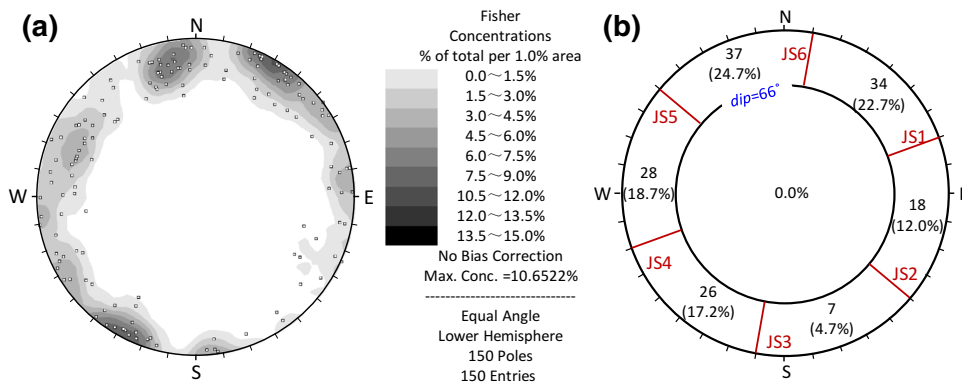


Fig. 9 pole and contour plots diagram and grouping features of columnar joints. **a** Pole and contour plots diagram of columnar joints; **b** columnar joint grouping



The pole distributions are discrete and do not have obvious boundaries between dominant joint sets. In addition, the column cross-sections generally have no more than six sides. Therefore, columnar joints are divided into six joint sets with 60° intervals for the quantitative description and analysis of joint stochastic properties to reflect the variable cross-sectional characteristics (Fig. 9b). The different sample sizes of the joint sets are used to describe the composite characteristics of multifarious column cross-section polygons.

Statistical characteristics of column diameters

The column diameter not only controls the size of columns, but also the cutting density of columnar joints. For the sake

of obtaining the actual column diameter, measurement information is modified based on trace features exposed on the tunnel walls, where one of the two column planes that intersect the wall is completely exposed. The trace of another incompletely exposed plane is assumed to bisect the exposed joint plane, as illustrated in Fig. 8b and c. An average correction factor η based on regular quadrilateral, pentagonal, and hexagonal columns is computed to amend the trace spacing d to obtain the column diameter D , expressed in Table 1, according to their geometrical relationship in Fig. 8b. To determine the optimal probability density distribution, the column diameters are tested with the Kolmogorov–Smirnov (K–S) distribution hypothesis testing method at 5% significance level. Analysis of the 190 data points of column diameters reveals that diameters

Table 1 Correction factors of the column diameter

Cross-section shape	Regular quadrangle	Regular pentagon	Regular hexagon	Actual shape
$\eta (D/d)$	1.26	1.17	1.11	1.18

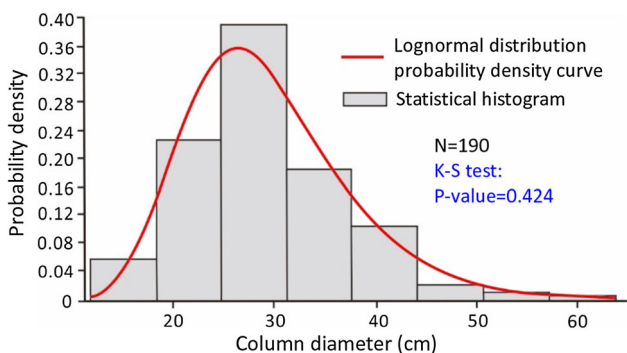


Fig. 10 Statistical histogram of column diameters obtained with UDSLM

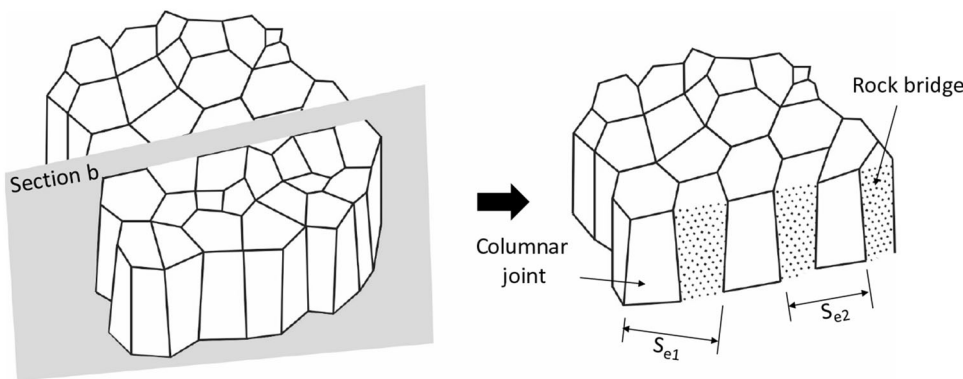
are mainly in the range of 15–35 cm while obeying a lognormal distribution (Fig. 10).

The CJB could be interpreted as being cut by six discontinuous joint sets, as shown in Fig. 11. The average persistence ratio of the regular quadrilateral and hexagon, 5/12, is used to approximate the persistence ratio of columnar joints mainly comprising quadrilaterals, pentagons, and hexagons, since a pentagon cannot individually constitute a closed cross-section and its form is between the quadrilateral and hexagon. The average spacing of columnar joints is scaled with the ratio of each joint set sample size to the average sample size of all joint sets, to quantify the cut spacing of columnar joints in different directions and to express the composite characteristic of multifarious polygons, as summarized by

$$S_{ei} = \frac{N_i}{N_u} \cdot S_u \approx \frac{N_i}{N_u} \cdot 2D, \tag{2}$$

where S_{ei} is the spacing of the i th columnar joint set, for $i = 1, 2, \dots, 6$, S_u is the average spacing of the six columnar joint sets, N_i is the measured sample number of the i th

Fig. 11 Spacing and persistence ratio of columnar joint sets



columnar joint set, and N_u is the average measured sample number of the six columnar joint sets.

Geometrical characteristic of internal joints

CJB internal joints are well developed in the dam foundation. The geometric features are strongly linked with the disturbance, weathering, alteration, and time effects as described in “Evolution of internal joint spacing”. Internal joints have a discernible impact on the mechanical properties of the rock mass. The large-area exposed internal joints near the dam foundation surface are measured to study their geometrical characteristics (Fig. 12). The diameter d_v of blocks cut by the ISDJ sets is 1–11 cm, with most falling in the range of 2.5–5.5 cm. The average diameter of the cutting blocks is 4.6 cm. A K–S testing reveals the lognormal distribution is the optimal probability distribution for describing the statistical properties of the block diameter (Fig. 13a). Figure 13b implies that quadrilateral is the most common block form. The IGDJ spacing S_h is 0.18–5.8 cm with most falling in the range of 0.5–2.5 cm, and the average spacing is 1.36 cm, while also obeying a lognormal distribution according to K–S testing (Fig. 13c).

Site validation of CJB specimens

To reveal the CJB structural characteristics in an intuitive and comprehensive way, specimens of 0.5 m edge length and 1.0 m height excavated artificially at the dam site were dismantled. The fully exposed columnar joints were then measured to verify the rationality and validity of the survey methods described above.

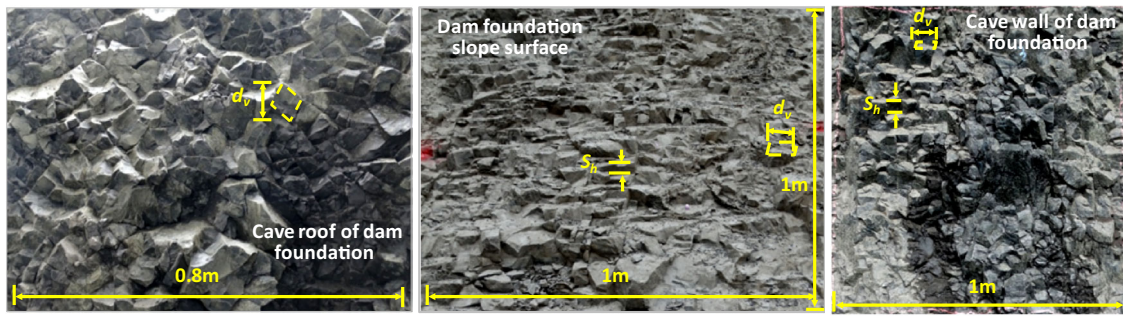


Fig. 12 Measurement of internal joints inside CJB

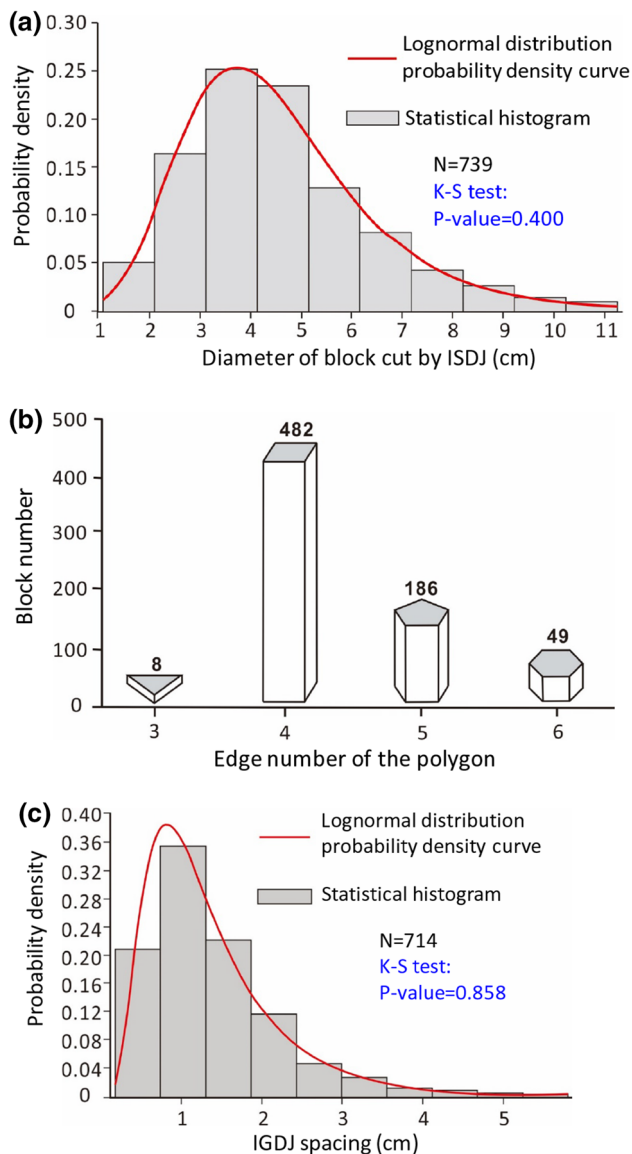


Fig. 13 Geometrical statistical features of internal joints. **a** Statistical features of block diameters cut by ISDJ; **b** block form cut by ISDJ; **c** Statistical features of IGDJ spacing

Validation of columnar joints

According to the surface morphology of columnar joints, the cuboid specimens were gradually dismantled along the joints after careful observation and identification to reveal intact columns. The attitudes of every exposed columnar joint and the diameters of every column were measured during this process (Fig. 14).

Pole and contour plots diagram for the intact columns are shown in Fig. 15a. The 360° heterogeneous distribution of poles confirms the non-uniformity of column cross-section shapes and the variability of the cross-section size of the same column along the column axis direction. The sample distribution proportions of the six joint sets are quantitatively compared with the results of the incomplete exposed columns measured with UDSLM (see Fig. 15b). The comparison shows that certain differences exist between the absolute size of the sample distribution proportions of the same joint set, because of the large difference in the total number of the joints for statistical analysis. However, the relative size of the proportions of different joint sets are almost consistent, which illustrates the measurement result with UDSLM is representative. The concentrated distribution range of the columnar joint tendency can well reflect the dumping orientation of the columns. The consistency of the concentrated distribution range of the columnar joint tendency, $250^\circ\text{--}70^\circ$, between the results of UDSLM and direct measurement further validates the effectiveness of the UDSLM method. In addition, the dip angle range of columnar joints of intact columns of $68^\circ\text{--}90^\circ$ is in good agreement with the range of the results of UDSLM listed in Fig. 9b. Meanwhile, Fig. 16 indicates that the diameters of intact columns also follow the lognormal distribution, and are mainly distributed in the range of 13–35 cm, which coincides well with the corrected diameters obtained through UDSLM. Therefore, the UDSLM is an effective and reasonable method to obtain large amounts of sample data of columnar joints for the purpose of reflecting the actual morphology.

Fig. 14 Measurement of intact columns in cuboid specimens. **a** The undivided cuboid specimen; **b** attitude measurements of columnar joints; **c** diameter measurement of intact columns

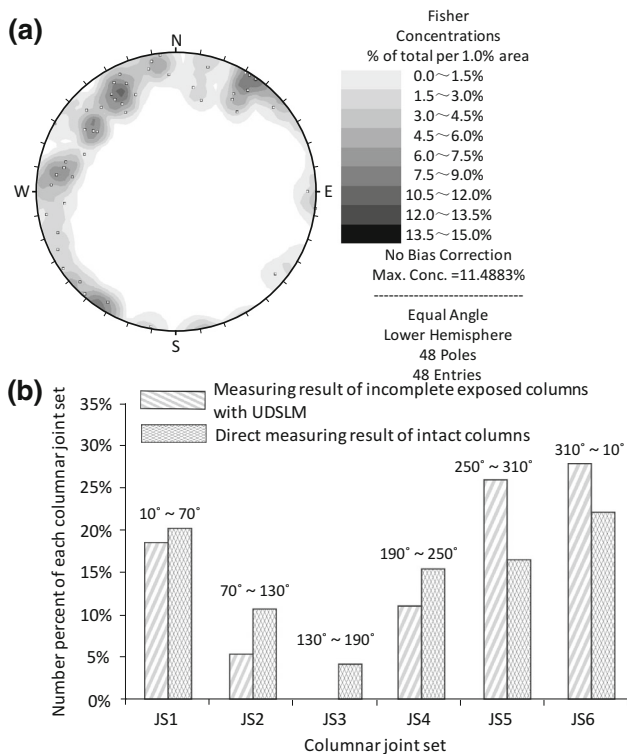
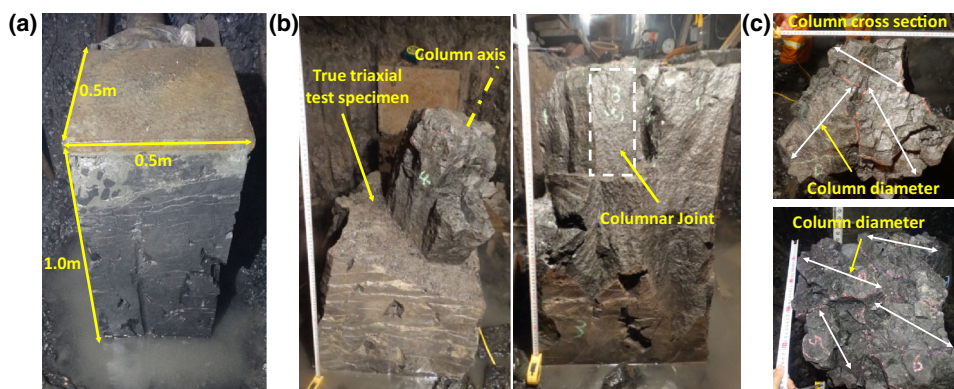


Fig. 15 Geometrical distribution features of columnar joints in intact columns. **a** Pole and contour plots diagram of columnar joints; **b** Comparison between measured results of the incomplete exposed columns with UDSLM and the intact columns

Validation of internal joints

The upper surface of the specimen is flush with the floor of the cave. Joint density on the side surfaces of the specimens clearly shows the effect of evolution on the spacing of internal joints, as shown in Fig. 17a. The spacing of the internal joints increases and the specimen is more integrated from the upper surface to the bottom, as the degree of unloading disturbance gradually diminishes. In the local alteration part, spacing is clearly reduced, especially for IGDJ spacing. Figure 17b shows the dispersion state of the

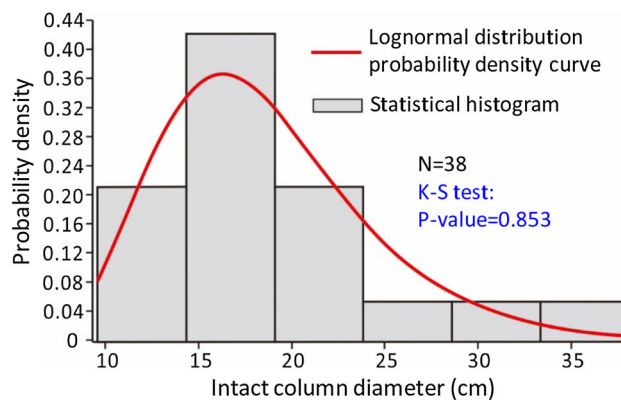


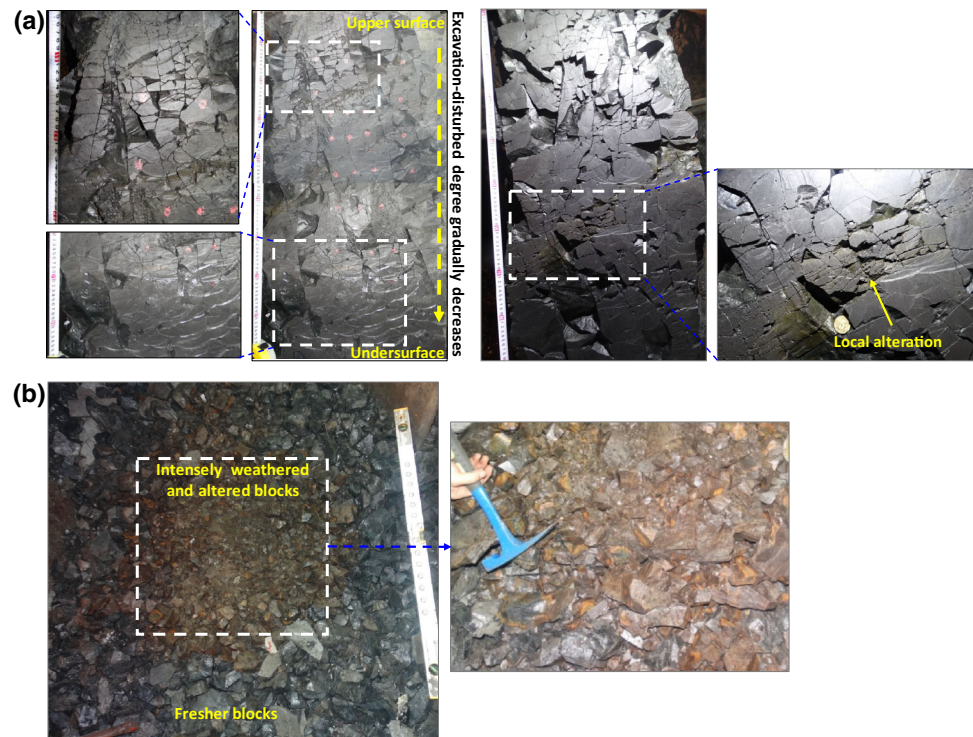
Fig. 16 Statistical histogram of intact column diameter

specimen after complete dismantlement. The size of naturally scattered blocks from the strongly weathered and altered CJB is significantly smaller than blocks from the fresher rock, which further strengthens the evidence that weathering and alteration contributes to the visible appearance and opening of internal joints.

Deformation characteristics

The characteristics of the columnar joint network determine the CJB anisotropic deformation (Shan and Di 2013). However, it is a challenging task to build a rock model containing the whole objective columnar joint system for direct evaluation of the CJB deformation anisotropy. Therefore, there is an urgent need for a sample index to describe the complicated space joint network. The crack tensor F proposed by Oda (1982) comprehensively and quantitatively expresses geometrical features, including density, size, and orientation of crack networks in a tensor form [see Eq. (3)] (Oda et al. 1984; Oda 1986; Oda et al. 1993), while offering a good theoretical base for expressing the integrated features of joint networks. Crack tensor theory is a promising approach to study the deformation of

Fig. 17 Evolution of internal joints in the cuboid specimens. **a** Spacing characteristic of internal joints on side surfaces of the specimens; **b** naturally scattered blocks of the specimen after dismantlement



a columnar joint system characterized by high joint density, complex joint types, and significant structural characteristics.

$$\mathbf{F} = \frac{\pi\rho}{4} \int_0^\infty \int_\Omega r^3 \mathbf{n} \otimes \mathbf{n} \otimes \dots \otimes \mathbf{n} E(\mathbf{n}, r) d\Omega dr, \quad (3)$$

where ρ is the volume density of cracks defined by $\rho = m^{(V)}/V$, $m^{(V)}$ is the number of cracks with centroids located inside a volume V , r is the diameter of a crack, the shape of which is assumed as an equivalently thin disc, \mathbf{n} is the unit direction vector of the crack, $E(\mathbf{n}, r)$ is the joint probability density function of \mathbf{n} and r , and Ω is the whole solid angle (4π).

With reference to the idea of the crack tensor, the geometric attributes of the columnar joint system—density, size, and orientation—are combined by means of probability integral and tensor product of the joint position vectors. The columnar joint tensor \mathbf{F}_{CJ} in a second-order tensor form is established to describe the spatial geometric features of a columnar joint network [see Eq. (4)], which considers the stochastic characteristics and could realize the space decomposition of geometric features.

$$\mathbf{F}_{CJ} = \frac{\pi\rho}{4} \int_\Omega \int_0^\infty r^2 \cdot \mathbf{n} \otimes \mathbf{n} \cdot E(r, \mathbf{n}) dr d\Omega. \quad (4)$$

For fresh or weakly weathered CJB with better integrity, the deformation of the rock mass is mainly controlled by the columnar joints. Combined with the special column structure and the measurable geometry parameters of the

columnar joints in “Geometric characteristics of columnar joints”, \mathbf{F}_{CJ} can be translated into (Cui et al. 2016)

$$\mathbf{F}_{CJ} = \sum_{i=1}^{N=6} \int_\Omega \int_0^\infty \frac{1}{S_{ei}} \cdot p \cdot \mathbf{n} \otimes \mathbf{n} \cdot E(S_{ei}) \cdot E(\mathbf{n}) dS_{ei} d\Omega. \quad (5)$$

The columnar joint tensor [see Eq. (6)] is acquired by substituting the columnar joint orientation, spacing and the persistence ratio analyzed in “Geometric characteristics of columnar joints” into Eq. (5). The eigenvalues and eigenvectors of the columnar joint tensor are presented in Eqs. (7) and (8), respectively.

$$\mathbf{F}_{CJ} = \begin{bmatrix} 4.763 & 0.548 & -0.256 \\ 0.548 & 5.249 & 0.544 \\ -0.256 & 0.544 & 0.209 \end{bmatrix}, \quad (6)$$

$$T_1 = 0.129, \quad T_2 = 4.467, \quad T_3 = 5.625, \quad (7)$$

$$\begin{aligned} \mathbf{v}_1 &= (0.068, -0.113, 0.991), \\ \mathbf{v}_2 &= (-0.850, 0.514, 0.117), \\ \mathbf{v}_3 &= (-0.523, -0.850, -0.061). \end{aligned} \quad (8)$$

The eigenvectors and eigenvalues of the second-order columnar joint tensor reflect the principal features of the spatial distribution of the columnar joint network, which is consistent with the controlled orientation and spatial deformation ability for the orthogonal columnar joint system. The corresponding orientation of eigenvector \mathbf{v}_1 in Eq. (8) is $137^\circ \angle 82^\circ$, which is approximately in agreement

with the orientation of the column axis. In this axis direction, the eigenvalue T_1 is close to nil, which indicates the deformation modulus in this direction is approximately equal to the intact rock. The plane determined by the eigenvectors v_2 and v_3 is perpendicular to the column axis.

According to the superposition principle under the linear elastic condition, the rock mass cut by three, or more than three, uniformly distributed joint sets with the same geometric characteristics possesses transversely isotropic deformation properties, which can be obtained by Eq. (9), namely, an equal elastic modulus along different directions of the same plane parallel to the transversely isotropic plane. Therefore, the deformation properties of a columnar jointed rock mass composed of regular hexagonal prisms and pentagonal prisms can be considered as the rock mass cut by three and five uniform distributed joint sets represented as transversely isotropic.

$$\frac{1}{E_x} = \frac{1}{E} + \sum_{i=1}^N \left[\frac{\cos^2 \alpha_i}{S_i} \left(\frac{\cos^2 \alpha_i}{k_{ni}} + \frac{\sin^2 \alpha_i}{k_{si}} \right) \right], \tag{9}$$

where E_x is the elastic modulus of the jointed rock mass in the specific research direction, and E is the elastic modulus of the intact rock. Here, S_i , k_{ni} and k_{si} are the spacing, normal stiffness and shear stiffness of the i th joint set, respectively; α_i is the angle between the normal vector of the joint set and the specific research direction of the elastic modulus.

The structural characteristics of the columnar jointed rock mass determine its potentially transversely isotropic properties for a transversely isotropic plane perpendicular to the column axis. The columnar joint tensor establishes a quantitative method to evaluate the structural properties of a columnar jointed rock mass. According to the orientation of the eigenvectors in Eq. (8), the T_2 and T_3 that reflect the distributed density of the columnar joints in the direction perpendicular to the column axis are compared to evaluate the uniformly distributed degree of columnar joint sets and determine the anisotropic property of the rock mass. Because the T_2 and T_3 in Eq. (7) are not strictly equal, the columnar joint rock mass is a general anisotropic body. However, as T_2 is approximately equal to T_3 , the deformation of columnar jointed rock mass can be considered to be approximately transversely isotropic. In addition, the relative size of T_1 and T_2 (or T_3) embodies the divergence degree of rock mass deformability between the transverse isotropic plane and the direction perpendicular to it.

Internal joints have a greater impact on the deformation of the rock mass after weathering and disturbance. The occurrences of ISDJ and columnar joints have a corresponding relationship, as described in “[Speculation on the formation mechanism](#)”. In that sense, the ISDJ occurrence could be approximately described with the occurrence of

columnar joints. ISDJ and IGDJ weaken the anti-distortion capacities of the direction parallel to and perpendicular to the transversely isotropic plane. According to the property of characteristic decomposition, the evolution of internal joint spacing will not change the principal deformation orientation of the rock mass if the ISDJ and IGDJ cut the rock mass orthogonally. IGDJ spacing can be as low as 1–2 mm. The CJB has distinct lamellar features and a potential cracking ability in the column-axis direction. With the intensification of weathering and disturbance, the reduction degree of the internal joint spacing controls the difference of the relative deformation ability in the directions parallel to and perpendicular to the transversely isotropic plane, as well as the evolution of the columnar joint tensor. Thus, CJB deformation is inconsistent at different weathering and disturbance states. Field-test will be a relatively reasonable and reliable method to estimate deformation parameters for the CJB in weathering and disturbance zones influenced by the density, aperture, and weathering degree of the joint wall of several types of joints.

Discussion

The intensive development of internal joints plays an important role in the stability of disturbed CJB in the left-bank dam foundation at Baihetan. The influence of structural characteristics on the engineering structure stability need to be further emphasized and discussed.

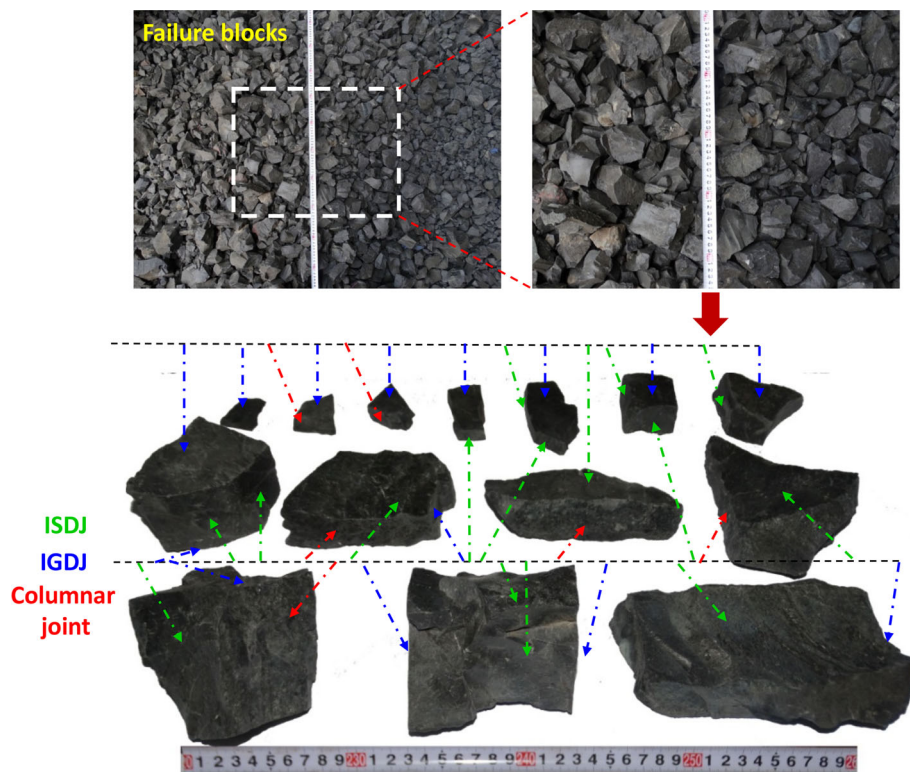
As expressed in Eq. (10), the joint quantity and type of internal joints governing the rock mass deformation and fracture are constantly changing, as the evolution of the visible spacing of internal joints. However, the evolution effect cannot be quantitatively represented and embedded in the constitutive equation. For CJB with irregular column structures and developed tensile fractures, geological surveys, and monitoring must be carried out to define clearly the extent of the weathering, disturbance state, master joint type, and relevant geometric characteristics, which are the foundation for accurate evaluation of CJB deformation and failure behavior.

$$S_v = f(DE, WE, TE), \tag{10}$$

where S_v is the spacing of visible internal joints, DE is the disturbance degree, WE is the extent of weathering and alteration, and TE is the time effect.

The developed joints in CJB, especially the intensive internal joints, and their regular orientation characteristics result in the block-failure behavior of the rock mass near the excavation surface. The rock mass breaks along the joints because of the intensive developed joints and the high strength of the intact basalt. Under different degrees

Fig. 18 Characteristics of scattered blocks of damaged CJB



of external disturbance, the spacing of internal joints is varied. As the different kinds of joints constitute the surfaces of failure blocks, the failure blocks are variable in size, as shown in Fig. 18. A smaller spacing of internal joints is accompanied by a higher cracking degree and a weaker carrying capacity of the rock mass. Therefore, support measures should concentrate on decreasing weathering and disturbance and providing timely support to restrain the cracking depth and extent.

Conclusions

Detailed field investigations of CJB in the Baihetan left-bank dam foundation have been reasonably extrapolated and comprehensively analyzed to reveal the structure, deformation, and failure characteristics from the formation mechanism to the actual exposed state.

The CJB is obviously partitioned and characterized by irregular column shapes, complex joint surfaces, and an intensive development of internal joints at the dam foundation surface. The CJB is cut into a typical mosaic block structure by columnar joints, IGDJ, and ISDJ. On the basis of a contraction hypothesis, temperature gradient variations and geometric control boundaries in the joint formation process determine the geometric features of internal joints, which present evident evolution effects, especially for the

IGDJ. As weathering, alteration, and disturbance intensify, the visible spacing of the internal joints decreases.

An UDSLM is put forward to gather large-sample geometric information on the multidirectional columnar joints when the exposed area of columns in the direction perpendicular to their axis is limited. The composite characteristics of multifarious polygons, variable cross-section characteristics of columns, and omnidirectional distributions of columnar joints were well reflected by the results of measurements, providing an effective way to combine the actual geometric features of in situ columnar joints and theoretical calculations. The soundness of this method is verified by the measured results of columnar joints in intact columns revealed by dismantling cuboid specimens.

The columnar joint tensor is established based on the objectively measured data of a non-persistent multiset and multidirectional joint network with UDSLM, and by drawing on the crack tensor theory. The eigenvectors of the joint tensor are consistent with the principal directions of equivalent deformation. The relative size of the eigenvalues reveals the deformation property of CJB to be approximately transversely isotropic, which quantitatively describe the distribution characteristics of columnar joint systems in different evolution states of the CJB. The intensively developed internal joints indicate that CJB failure behavior possesses prominent block cracking characteristics and the visible spacing of internal joints

determines the cracking lumpiness, as well as the carrying capacity of the rock mass.

Acknowledgements The authors gratefully acknowledge the financial support from the State Key Research Development Program of China (Grant No. 2016YFC0600707), National Natural Science Foundation of China (Grant No. 51379202 and 41372315). In particular, authors also wish to thank China Three Gorges Project Corporation, Huadong Engineering Co. LTD., Power China and Changjiang Rive Scientific Institute of Changjiang Water Resources Commission for their field investigation supports.

References

- Barton N, Quadros E (2014) Anisotropy is everywhere, to see, to measure, and to model. *Rock Mech Rock Eng* 48(4):1323–1339
- Brady BH, Brown ET (2013) *Rock mechanics: for underground mining*. Springer Science and Business Media
- Budkewitsch P, Robin PY (1994) Modelling the evolution of columnar joints. *J Volcanol Geoth Res* 59(3):219–239
- Cui J, Jiang Q, Feng XT, Li SJ, Gao H, Li SJ (2016) Equivalent elastic compliance tensor for rock mass with multiple persistent joint sets: exact derivation via modified crack tensor. *J Cent South Univ* 23(6):1486–1507
- Dai F, Li B, Xu NW, Fan YL, Xu J, Liu J (2016) Microseismic characteristic analysis of underground powerhouse at Baihetan hydropower station subjected to excavation. *Chin J Rock Mech Eng* 35(4):692–703 (in Chinese)
- Degraff JM, Aydin A (1993) Effect of thermal regime on growth increment and spacing of contraction joints in basaltic lava. *J Geophys Res Solid Earth* 98(B4):6411–6430
- Di SJ, Xu WY, Ning Y, Wang W, Wu GY (2011a) Macro-mechanical properties of columnar jointed basaltic rock masses. *J Cent South Univ Technol* 18:2143–2149
- Di SJ, Xu WY, Wang W, Shi AC (2011b) Transversely isotropic constitutive properties of a columnar jointed rock mass. *J China Univ Min Technol* 40(6):881–887 (in Chinese)
- Di SJ, Xu WY, Shan ZG (2013) Study of anisotropic equivalent elastic parameters of jointed rock mass. *Rock Soil Mech* 34(3):696–702 (in Chinese)
- Feng XT, Jiang Q, Li SJ et al (2015) Aging relaxation test and feedback analysis of anchor effect for columnar jointed rock mass in left-bank dam foundation of Baihetan Hydropower Station in Jinsha river. Institute of Rock and Soil Mechanics, Chinese Academy of Sciences, China (in Chinese)
- Goehring L (2013) Evolving fracture patterns: columnar joints, mud cracks and polygonal terrain. *Philos Trans R Soc Lond A Math Phys Eng Sci* 371(2014):20120353
- Goehring L, Mahadevan L, Morris SW (2009) Nonequilibrium scale selection mechanism for columnar jointing. *Proc Natl Acad Sci* 106(2):387–392
- Grossenbacher KA, McDuffie SM (1995) Conductive cooling of lava: columnar joint diameter and stria width as functions of cooling rate and thermal gradient. *J Volcanol Geoth Res* 69(1):95–103
- Hetényi G, Taisne B, Garel F, Médard É, Bosshard S, Mattsson HB (2012) Scales of columnar jointing in igneous rocks: field measurements and controlling factors. *Bull Volc* 74(2):457–482
- Hudson JA, Harrison JP (2000) *Engineering rock mechanics—an introduction to the principles*. Pergamon, London
- Hudson J, Priest S (1983) Discontinuity frequency in rock masses. *Int J Rock Mech Min Sci Geomech Abstr* 20(2):73–89
- Hull D, Caddock B (1999) Simulation of prismatic cracking of cooling basalt lava flows by the drying of sol-gels. *J Mater Sci* 34(23):5707–5720
- Jiang Q, Feng XT, Hatzor YH, Hao XJ, Li SJ (2014) Mechanical anisotropy of columnar jointed basalts: an example from the Baihetan hydropower station, China. *Eng Geol* 175:35–45
- Jin CY, Yang CX, Fang D, Xu S (2015) Study on the failure mechanism of basalts with columnar joints in the unloading process on the basis of an experimental cavity. *Rock Mech Rock Eng* 48(3):1275–1288
- Liu SG, Chi YX, Wang SJ, Liu HN, Shi AC (2009) Size effect on shear strength of basalt rock mass with columnar joints. *J Eng Geol* 17(3):367–370 (in Chinese)
- Müller G (1998a) Experimental simulation of basalt columns. *J Volcanol Geoth Res* 86(1):93–96
- Müller G (1998b) Starch columns: analog model for basalt columns. *J Geophys Res Solid Earth* (1978–2012) 103(B7):15239–15253
- Oda M (1982) Fabric tensor for discontinuous geological materials. *Soils Found* 22(4):96–108
- Oda M (1986) A stereological study on crack geometry of discontinuous rock masses. In: *Proceedings of the first international symposium for science on form*. KTK Scientific Publisher, Tokyo, pp 183–189
- Oda M, Suzuki K, Maeshibu T (1984) Elastic compliance for rock-like materials with random cracks. *Soils Found* 24(3):27–40
- Oda M, Yamabe T, Ishizuka Y, Kumasaka H, Tada H, Kimura K (1993) Elastic stress and strain in jointed rock masses by means of crack tensor analysis. *Rock Mech Rock Eng* 26(2):89–112
- Phillips JC, Humphreys MCS, Daniels KA, Brown RJ, Witham F (2013) The formation of columnar joints produced by cooling in basalt at Staffa, Scotland. *Bull Volcanol* 75(6):1–17
- Reiter M, Barroll MW, Minier J, Clarkson G (1987) Thermo-mechanical model for incremental fracturing in cooling lava flows. *Tectonophysics* 142(2):241–260
- Salazar F, Toledo MA, Oñate E, Suárez B (2016) Interpretation of dam deformation and leakage with boosted regression trees. *Eng Struct* 119:230–251
- Shan ZG, Di SJ (2013) Loading-unloading test analysis of anisotropic columnar jointed basalts. *J Zhejiang Univ Sci A* 14(8):603–614
- Singh M, Rao K, Ramamurthy T (2002) Strength and deformational behaviour of a jointed rock mass. *Rock Mech Rock Eng* 35(1):45–64
- Spry A (1962) The origin of columnar jointing, particularly in basalt flows. *J Geol Soc Aust* 8(2):191–216
- Sun GZ (1993) On the theory of structure-controlled rock mass. *J Eng Geol* 1(1):14–18 (in Chinese)
- Wang SJ (2009) Geological of rock and its deduction for rock mechanics. *Chin J Rock Mech Eng* 28(3):433–450 (in Chinese)
- Xu WY, Zheng WT, Ning Y, Meng GT, Wu GY, Shi AC (2010) 3D anisotropic numerical analysis of rock mass with columnar joints for dam foundation. *Rock Soil Mech* 31(3):949–955 (in Chinese)
- Xu JR, Shi AC, Chou CY et al (2015a) Engineering geology report for left-bank and riverbed dam foundation excavation treatment during detail design phase of construction of Baihetan Hydropower Station in Jinsha river. China Hydropower Electric Consultant Corporation, Hangzhou, East China Investigation and Design Institute, China (in Chinese)
- Xu JR, Shi AC, Chou CY et al (2015b) Engineering geology report for excavation treatment of columnar jointed basalt dam foundation during detail design phase of construction of Baihetan Hydropower Station in Jinsha river. China Hydropower Electric Consultant Corporation, Hangzhou, East China Investigation and Design Institute, China (in Chinese)
- Yang Q, Liu Y, Chen Y, Zhou W (2010) Stability and reinforcement analyses of high arch dams by considering deformation effects. *J Rock Mech Geotech Eng* 2(4):305–313
- Zarzicky J (1982) *Les verres et l'état vitreux*. Manson, Paris

- Zheng WT, Xu WY, Yan DX, Ji H (2011) A three-dimensional modeling method for irregular columnar joints based on voronoi graphics theory. *Applied informatics and communication*. Springer, Berlin, Heidelberg, pp 62–69
- Zhu DJ (2010) Unloading effect and rapture zone distribution of columnar joints cavern. *J Zhejiang Univ (Eng Sci)* 44(10):1967–1973 (in Chinese)
- Zhu DJ, Yang LD, Cai YC (2009) Research on anisotropic characteristics and size effect of columnar jointed rock mass. *Chin J Rock Mech Eng* 28(7):1405–1414 (in Chinese)